

Identification of the young stellar clusters in the G345.5+1.5 Star-Forming Region

A. Khachatryan^{*1}, E. Nikoghosyan², D. Andreasyan², A. Samsonyan², N. Azatyan², V. Grigoryan¹,
and R. Simonyan²

¹Yerevan State University, Yerevan, Armenia

²Byurakan Astrophysical Observatory, Byurakan, Aragatsotn Province, Armenia

Abstract

Star-forming regions, their formation and evolution are a subject of active study. The subject of our research is the G345.5+1.5 region, which is composed of two dusty ring-like structures referred to as G345.45+1.5 and G345.10+1.35. The region is located at a distance of 1.8 kpc and classified as HII regions. According to previous studies, G345.45+1.5 could have been created by a supernova explosion represented by the 36.6 cm source J165920-400424 in its center. Despite the considerable interest, only a few works are devoted to this region, and there is very little information about its stellar population. Our work focuses specifically on the stellar population in this region. Using 2MASS astrometric and photometric data, we identified three well-defined clusters of young stellar objects (YSOs) in the vicinity of the IRAS 16561-4006, 16571-4029, and 16545-4012 sources.

Keywords: stars: formation, stars: pre-main sequence, stellar cluster: G345.5+1.5

1. Introduction

Even in our current era, star formation within the Galaxy continues (Ambartsumian, 1947). Regions of star formation, identified by dense molecular clouds that exhibit gravitational instability, serve as crucial sites where the complex interplay of physical forces initiates the birth of stellar objects. Thorough investigation of these regions is essential for enhancing our understanding of stellar evolution in general. Within these molecular clouds, dense regions form and initiate star formation as gas and dust collapse. The complex interaction of forces determines the location and movement of star-forming cores, impacting the later development of newborn stars (Lada & Lada, 2003). Therefore, the study of star formation regions serves multiple objectives. Firstly, it offers a window into the initial phases of stellar birth, providing insights into the physical conditions and dynamical processes governing the formation of protostellar cores. By employing high-resolution observations of molecular gas and dust, astronomers can delineate the hierarchical structure of star-forming regions and investigate the mechanisms driving their fragmentation and collapse. In turn, understanding the characteristics of young stellar populations is essential for deriving insights into star formation processes within parent molecular clouds.

The main goal of our work is to search for the stellar population in the G345.45+1.5 and G345.10+1.35 molecular clouds, which are part of the G345.5+1.5 star formation region (see Figure 1). These molecular clouds are located 1.8 kpc apart and classified as a single HII region (Figueira et al., 2019). They contain a significant number of IRAS sources (see right panel of Fig. 1). According to López-Calderón et al. (2016), the northern cloud, G345.45+1.5, could have been caused by a supernova explosion. This is supported by the bow-shock shape of the interstellar medium (ISM) in G345.10+1.35, which is clearly visible at the WISE 22 μm wavelength (see left panel of Fig. 1). To date, there are only a few studies on this star-forming region, resulting in limited information about its stellar population. On the other hand, understanding the properties of the stellar population, including spatial distribution, mass function, and evolutionary age spread, can provide clarity in understanding their formation and evolution.

The paper is organized as follows: Section 2 describes the data used; Section 3 presents the results obtained and their discussion: radial distribution of the surface stellar density and identification of young

*arman.khachatryan21@edu.y-su.am

stellar objects (YSOs) using colour-colour (c-c) diagrams. Finally, the conclusions drawn from the obtained results are presented in Section 5.

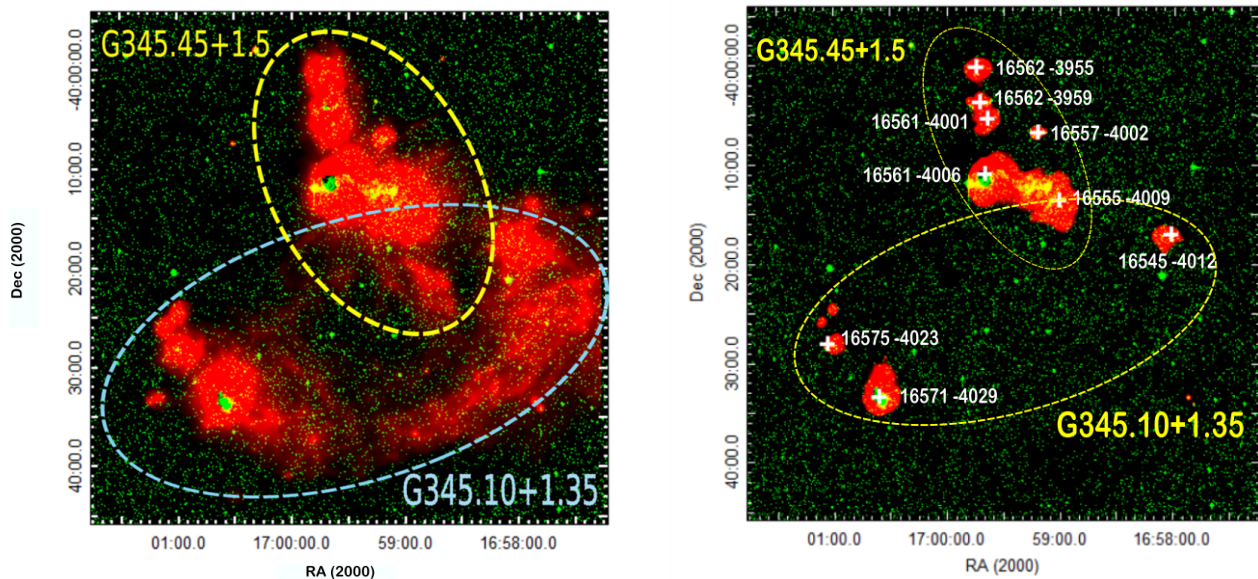


Figure 1. Colour-composite images of the G345.45+1.5 star formation region (green - 2MASS K and red-WISE 22 μm) with different contrast. The IRAS sources are marked by crosses and labeled on the right panel.

2. Used data

In our study, we used near- and mid-infrared (NIR and MIR, respectively) data. The first dataset comprises archival NIR photometric data in the J, H, and K bands of the Two Micron All-Sky Survey (2MASS) with a resolution of 2 arcsec/pix. The photometric limits for point sources with a 5σ signal-to-noise ratio 16.3 mag in the J band, 15.8 mag in the H band, and 15.0 mag in the K_s band. These limits are essential for studying the structure and composition of star-forming regions (Skrutskie et al., 2006).

Archival MIR observations were obtained from the Galactic Legacy Infrared Midplane Survey Extraordinary (GLIMPSE, Churchwell et al., 2009). These observations were conducted using the Infrared Array Camera (IRAC, Fazio et al., 2004) on the Spitzer Space Telescope. The four IRAC bands are centred at ~ 3.6 , 4.5, 5.8, and 8.0 μm with a resolution of 0.6 arcsec/pix.

3. Results and discussion

Figure 1 shows that stellar population in the G345.5+1.5 formation region has a multicomponent, hierarchical structure, making its detailed study of considerable interest. The point sources are mostly concentrated around the IRAS sources, forming three well-defined clusters. We named these clusters as IRAS 16575-4023 & 16571-4029, G345.45+1.5, IRAS 16545-4012 (see Fig. 2).

3.1. Radial surface stellar density distribution

The first step of our work is to confirm the existence of these clusters. For this purpose, we constructed the radial density distributions of the point sources from 2MASS database with K_s mag < 15.0 in areas, which exceed the dimensions of the bright nebulae in the IRAS 16575-4023 & 16571-4029, G345.45+1.5, IRAS 16545-4012 regions. These areas are marked by white circles in Figure 2. The centers of circles are given in Table 1. In the IRAS 16575-4023 & 16571-4029 and G345.45+1.5 region, we used the geometric centers, while for IRAS 16545-4012, the center coincides with the IRAS source coordinates. Table 1 also contains the radii of the searching areas and clusters (see text below).

To determine the surface density of point source, we divided the regions into rings of a certain width and then divided the number of stars in each ring by the surface of the ring. We used the standard error of the

number of stars in the rings as a measure of uncertainty. The stellar density distributions for the clusters are presented in the Figure 3. The radial density distributions show a well-defined concentrations of stars around the IRAS sources, confirming the the existence of clusters. Starting from radii of $8'$, $11'$, and $3'$ in the IRAS 16575-4023 & 16571-4029, G345.45+1.5, IRAS 16545-4012 regions, respectively, the stellar density does not exceed the average density of the field. These radii can be considered as the cluster radii. These regions are marked in yellow in Figure 2.

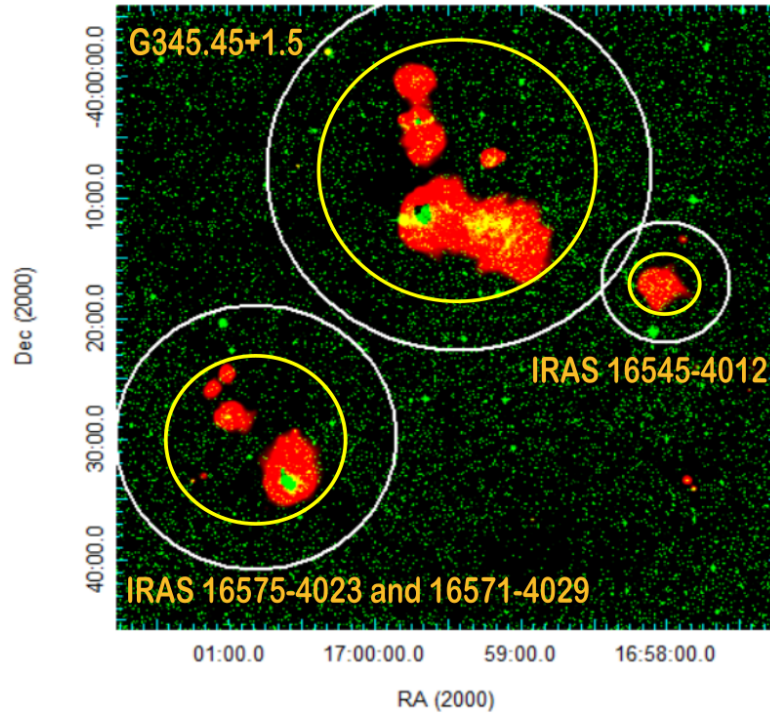


Figure 2. Colour-composite image of the G345.45+1.5 star (green - 2MASS and red - WISE $22\ \mu\text{m}$). The white circles define the region in which the radial distribution of stellar surface density was plotted. Yellow circles outline areas of increased density.

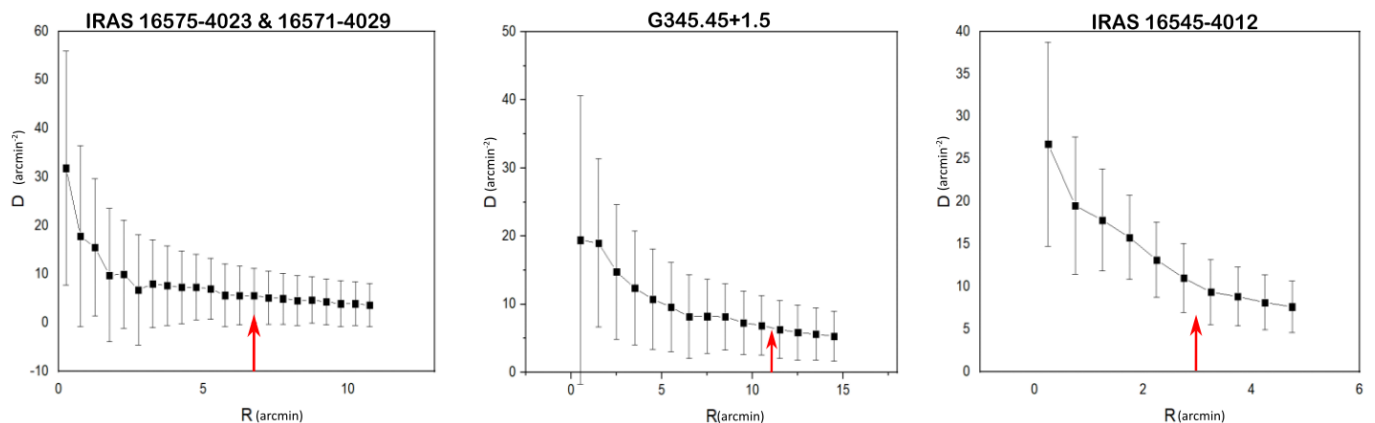


Figure 3. Radial distribution of surface stellar densities, with red arrows indicating the clusters' radii.

4. Colour-colour diagrams

When selecting potential cluster members from stars located in the direction of the molecular cloud, we assumed that most of the members of the considered active star-forming region are YSOs. One of the main observational characteristics of YSOs is an infrared (IR) excess due to the presence of circumstellar discs and envelopes (Hartmann, 2009, Lada & Lada, 2003). Furthermore, the measure of the IR excess in

Table 1. Coordinates of the centers and the radii of the searching areas and clusters

Cluster name	RA (2000)	Dec (2000)	R of searching area	R of cluster
IRAS 16575-4023 & 16571-4029	17:00:48	-40:30:00	11'	6'
G345.45+1.5	16:59:25	-40:07:50	15'	10'
IRAS 16545-4012	16:58:01.0	-40:17:09	5'	3'

the NIR and/or MIR ranges can be used to characterise the evolutionary stage of a YSO (Class I and II). Therefore, YSO candidates can be identified based on their IR colour indices, i. e., their position in *c-c* IR diagrams. Numerous studies have provided theoretical justifications that explain the placement of YSOs in the *c-c* diagrams, correlating specific positions with different evolutionary stages. For our analysis we employed three distinct *c-c* diagrams for IR point sources within the clusters' radii:

- (J–H) vs. (H–K) *c-c* NIR diagram (Hernández et al., 2005, Lada & Adams, 1992, Meyer et al., 1997);
- K–[3.6] vs. [3.6]–[4.5] *c-c* diagram, which combines NIR and MIR photometric data (Allen et al., 2007);
- MIR [3.6]–[4.5] vs. [5.8]–[8.0] *c-c* MIR diagram (Allen et al., 2007).

Aside from YSOs, other objects can also display an IR excess and may be mistakenly identified as YSOs. These objects include: (i) star-forming galaxies and narrow-line active galactic nuclei (AGNs), which exhibit increasing excesses at 5.8 and 8.0 μm due to hydro-carbon emissions; (ii) broad-line AGNs, whose IRAC colours closely resemble those of YSOs. To maintain the purity of our YSO sample, we excluded all point sources with colour indices typical of the aforementioned categories, as identified by Gutermuth et al. (2008). The positions of the point sources from 2MASS and GLIMPSE databases within the clusters' radii on the *c-c* diagrams are presented in Figures 4 and 5.

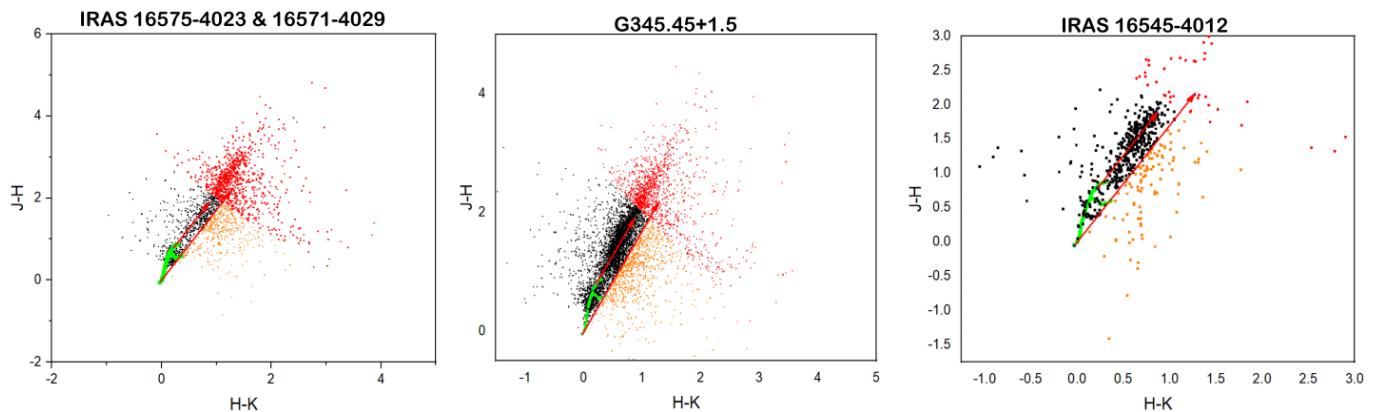


Figure 4. (J–H) versus (H–K) colour-colour diagrams for the clusters. The green curves represent the positions of dwarfs and giants (Bessell, 1988), converted to the CIT photometric system (Carpenter, 2001). The red vectors are reddening vectors reflecting interstellar absorption (Rieke et al., 1985). Objects with different evolutionary stages are marked by different colors: red for Class I with $J - K > 3$ (Lada & Adams, 1992), orange for objects with IR excess (Class I/II), and black for objects, which were not selected as potential YSOs.

The deviation of stars from the main sequence (MS) on the (J–H) vs. (H–K) *c-c* NIR diagram can have two reasons: the presence of an IR excess and interstellar absorption, which also leads to reddening of objects. However, in the latter case, the deviation from the MS will be directed along the reddening vectors. Therefore, the IR excess of objects to the right of the reddening vectors cannot arise solely from interstellar absorption; at least in part, their IR excess must be due to the presence of the disk and envelope surrounding them. Hence, objects to the right of the reddening vectors can be considered as YSO candidates. We also consider objects with $J - K > 3$ as YSO candidates. According to Lada & Adams (1992), those objects may be considered as Class I evolutionary stage YSOs.

MIR wavelengths are also used to identify YSOs with different evolutionary stages. The positions of the stellar objects with different evolutionary stages based on the *Spritzer* IRAC photometric bands are well developed by Allen et al. (2007).

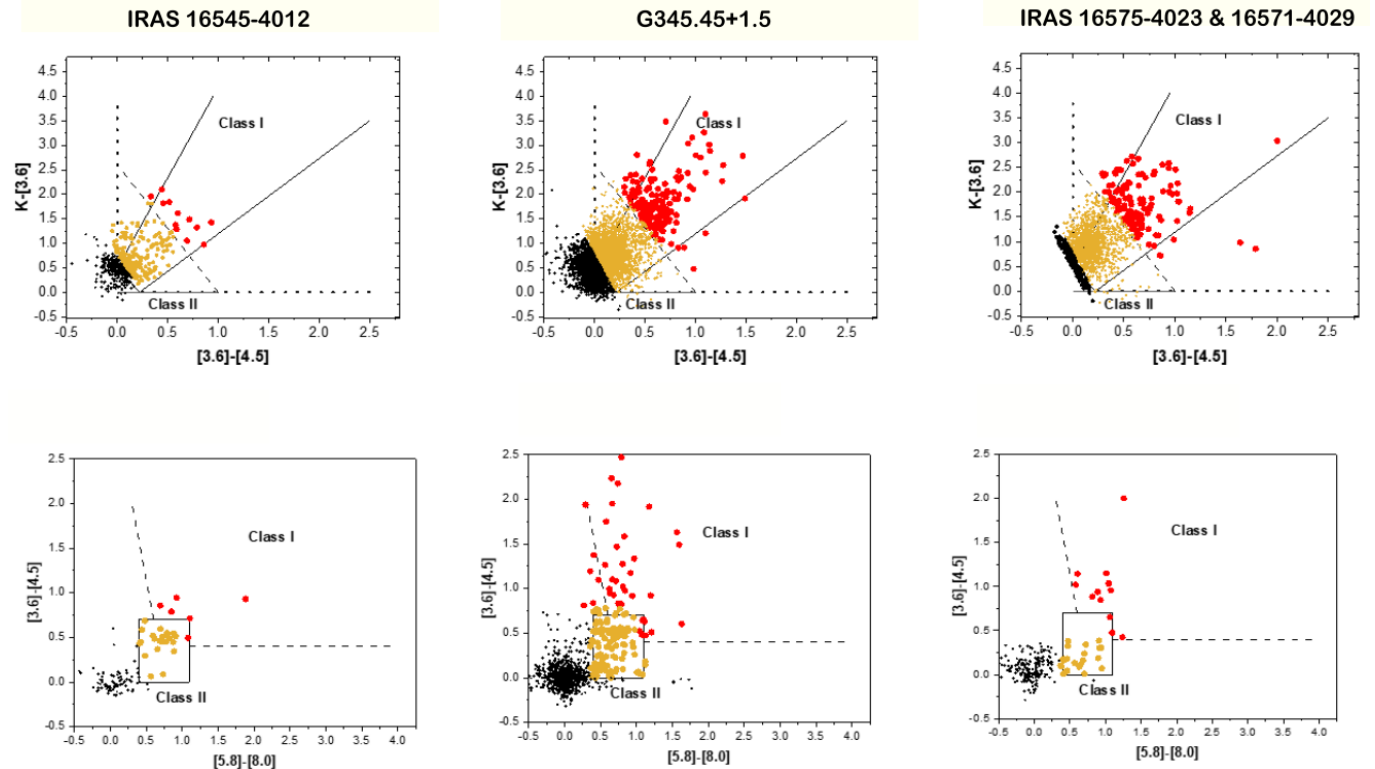


Figure 5. Colour–colour diagrams of the clusters. *Top panels*: $K-[3.6]$ versus $[3.6]-[4.5]$ diagrams and *bottom panels*: $[3.6]-[4.5]$ versus $[5.8]-[8.0]$ diagrams. In all diagrams, Classes I and II domains are separated by the dashed lines. All lines are from Allen et al. (2007). Objects with different evolutionary stages are marked by different colours: red for Class I, orange for Class II, and black for objects, which were not selected as potential YSOs.

Table 2. Number of identified YSOs at different stages of evolution

Cluster name	Class I	Class II
IRAS 16575-4023 & 16571-4029	8	118
G345.45+1.5	44	607
IRAS 16545-4012	6	67

Object selection based on photometric data alone cannot be considered very accurate for several reasons:

- There is a possibility that objects, which do not belong to the molecular cloud may be selected;
- Stellar objects with small NIR excesses are excluded from the selection;
- Young stars can be positioned differently relative to us, which can result in varying classifications across different wavebands.

To minimize the possibility of incorrect selection, we chose YSOs classified as IR excess objects in at least two diagrams. The final results for the identification of YSOs in clusters are given in Table 2. The significant number of identified YSOs in the clusters is further evidence that G345.45+1.5 is a very active star-forming region, deserving much more detailed study. Moreover, the number of YSOs directly depends on the size of the surrounding nebulae. This is most likely due to the fact that the greater mass of the ISM causes more active star formation. However, the percentage content of Class I YSOs in the clusters is almost the same (6–8%). Could this be a consequence of the fact that star formation in all three clusters was initiated simultaneously? This and other questions require further research.

5. Conclusion

The main goal of our work is to search for the young stellar population in the G345.45+1.5 and G345.10+1.35 molecular clouds, which are part of the G345.5+1.5 star formation region. For this pur-

pose we used NIR and MIR photometric data obtained from 2MASS and GLIMPSE databases. The point sources in the region are mostly concentrated around the IRAS sources, forming three well-defined clusters. We named these clusters as IRAS 16575-4023 & 16571-4029, G345.45+1.5, and IRAS 16545-4012.

The first step of our work is to confirm the existence of these clusters. For this purpose, we constructed the radial surface density distributions of the point sources from the 2MASS database with K_s mag < 15.0 in areas that exceed the dimensions of the bright nebulae in the clusters' regions. According the radial density distributions the radii of the clusters are $8'$, $11'$, and $3'$ for the IRAS 16575-4023 & 16571-4029, G345.45+1.5, and IRAS 16545-4012 regions, respectively.

For the identification of YSOs in the clusters, we used NIR and MIR colour indices. i.e. the position on the c-c diagrams of point sources within the clusters' radii. We used three c-c diagrams: (J-H) vs. (H-K), K-[3.6] vs. [3.6]-[4.5], and [3.6]-[4.5] vs. [5.8]-[8.0]. In total, we identify 850 YSOs, of which 58 are at Class I evolutionary stage. The significant number of identified YSOs in the clusters is further evidence that G345.45+1.5 is a very active star-forming region, deserving much more detailed study.

It is important to note that the selection of YSOs is only the initial stage of the overall research. The next step involves determining their parameters, specifically their masses and evolutionary ages, as well as the density and temperature of the ISM. These determinations will enable us to draw comprehensive conclusions about the entire star formation process in the region.

Acknowledgements

This work partially was made possible by a research grant number № 21AG-1C044 from Science Committee of Ministry of Education, Science, Culture and Sports RA. This publication makes use of data products from the Two Micron All Sky Survey, which is a joint project of the University of Massachusetts and the Infrared Processing and Analysis Center/California Institute of Technology, funded by the National Aeronautics and Space Administration and the National Science Foundation. We thank our colleagues in the GLIMPSE and MIPS GAL Spitzer Legacy Surveys. This publication also made use of data products from Herschel ESA space observatory.

References

- Allen L., et al., 2007, *Protostars and Planets V*, pp 361–376
- Ambartsumian V. A., 1947, *The Evolution of Stars and Astrophysics*. Cambridge University Press, Cambridge
- Bessell M. S., 1988, *Astronomy and Astrophysics Supplement Series*, 74, 109
- Carpenter J. M., 2001, *The Astronomical Journal*, 121, 3160
- Churchwell E., et al., 2009, *Publ. Astron. Soc. Pac.* , 121, 213
- Fazio G. G., et al., 2004, *Astrophys. J. Suppl. Ser.* , 154, 10
- Figueira M., López-Calderón C., Bronfman L., Zavagno A., Hervías-Caimapo C., Duronea N., Nyman L. Å., 2019, *Astron. Astrophys.* , 623, A141
- Gutermuth R. A., et al., 2008, *Astrophys. J.* , 674, 336
- Hartmann L., 2009, *Annual Review of Astronomy and Astrophysics*, 47, 565
- Hernández J., Calvet N., Hartmann L., Briceño C., Sicilia-Aguilar A., Berlind P., 2005, *Astron. J.* , 129, 856
- Lada C. J., Adams F. C., 1992, *The Astrophysical Journal*, 393, 278
- Lada C. J., Lada E. A., 2003, *Annual Review of Astronomy and Astrophysics*, 41, 57
- López-Calderón C., Bronfman L., Nyman L.-Å., Garay G., de Gregorio-Monsalvo I., Bergman P., 2016, *Astronomy & Astrophysics*, 595, A88
- Meyer M. R., Calvet N., Hillenbrand L. A., 1997, *Astron. J.* , 114, 288
- Rieke G. H., Lebofsky M. J., Low F. J., 1985, *The Astrophysical Journal*, 288, 618
- Skrutskie M. F., et al., 2006, *Astron. J.* , 131, 1163